2016
International Symposium on Power Electronics,
Electrical Drives, Automation and Motion

Control Techniques for Torque Ripple Minimization in Switched Reluctance Drives under Faults

Dubravka, P., Rafajdus, P., Makys, P.
Department of Power Electrical Systems
University of Zilina
Slovakia
pavol.rafajdus@fel.uniza.sk

Szabo, L.
Department of Electrical Machines and Drives
Technical University of Cluj-Napoca
Romania
Lorand.Szabo@emd.utcluj.ro

***Abstract*—This paper deals with comparison of several control techniques for torque ripple minimization in drives with switched reluctance motor (SRM) under fault operation mainly if one phase is open. These techniques are: hysteresis control of phase current, PWM control, phase current profiling and direct instantaneous torque control. The basic principles of these methods are described, SRM parameters investigations by means of Finite Element Method is presented, simulation analysis is carried out and several methods are compared with experimental ones.**

Keywords—switched reluctance motor, 3D FEM parametrical model, torque ripple minimization

I. INTRODUCTION

The Switched Reluctance Motor (SRM) belongs to the simplest electrical machines. SRM is characterized by robustness and the manufacturing costs are lower in comparison with others electrical machines [1]. The SRM has simple construction. It is electrical machine which has salient poles on both the rotor and the stator, see Fig. 1. Each phase comprises two or four coils wound on opposite stator poles and connected in series or parallel [2], [3]. It leads to the generation of the magnetic flux. The torque is produced by tendency of its moveable part (rotor) to move into a position where the inductance of the excited winding is maximized [4]. One of the biggest disadvantages of this motor is torque ripple caused by its double saliency on the stator and rotor. In many papers, some different techniques are used to minimize torque ripple during normal operation [5], [6].

In this motor also several faults can be occurred during its operation. These faults can be electrical and mechanical. The electrical faults could be: short circuit in one coil of a phase (all turns or some turns), a whole coil is bridged by a short circuit, the whole phase is short circuited, open circuit in one coil of a phase, one phase is opened, a short circuit between two different phases, a short circuit from one winding to ground [7], [8]. All of these faults can increase its torque ripple. In [9] **a fault-tolerant SRM drive with adaptive fuzzy logic controller providing smooth torque with minimum ripple under normal and fault conditions is described.**

This paper is mainly devoted to a SRM used as drive in electric vehicle. During its faulty state (when one phase is opened) the most important task is to get the car even at a lower speed to the nearest service station where it can be repaired. In [10], the research is focused on the comparative study of the current hysteresis control and direct instantaneous torque control (DITC) techniques.

In this paper a real SRM (three phase, 12/8, 540 V, 3000 rpm, 3700 W) is investigated from point of view torque ripple minimization during normal and fault (one phase is open) operation. Static parameters of the SRM are investigated by means of 2D and 3D FEM parametrical model and they are verified by measurement. Mathematical model of SRM is used for simulation of transient. Four control techniques for torque ripple minimization are described, simulated and experimental verified.

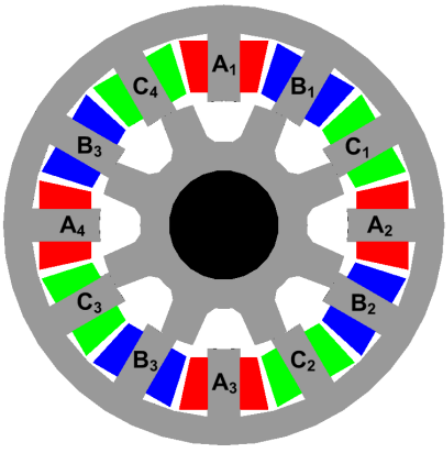

Fig. 1 The three phase SRM analyzed in this paper.

II. SRM STATIC PARAMETERS ANALYSIS

To be able solve and to simulate mathematical model of SRM, the input parameters are needed. These are static parameters of SRM as phase inductance, flux linkage and electromagnetic torque created by one phase. It must be noted, that all of these parameters depend on phase current and rotor position. There are several methods, how to analyze the static parameters of the SRM: analytical approach, FEM (2D, 3D) and measurements. The FEM analysis needs the following input data: geometrical dimensions of the machine, excitation current, material constants (winding conductivity and relative

978-1-5090-2067-6/16/$31.00 ©2016 IEEE

permeability, B-H curve of SRM ferromagnetic circuit material) and boundary conditions. The parametric 2D model of the SRM has been created in the FEMM 4.2 software and parametric 3D model in OPERA software. Detail analysis of these SRM static parameters can be seen in [14].

III. Mathematical model of SRM

On the base of static parameters analysis and their comparison, parameters obtained by means of 3D FEM are used in the mathematical model and in all simulations. Dynamic model of the SRM was created on the base of the next equations and by using a mathematical model, which enabled the calculation of the phase current, speed, voltage and dynamic torque.

The electromagnetic torque of SRM can be calculated from:

$$T_e = \frac{\partial \int_0^i \Psi di}{\partial \Theta}. \tag{1}$$

The voltage equation of one SRM phase is given as:

$$v = Ri + \frac{d\psi}{dt}. \tag{2}$$

where R is phase resistance, i is phase current and ψ is flux linkage. The flux linkage depends on both parameters: phase current and rotor position ($\psi = f(i, \Theta)$). Then

$$\frac{d\psi}{dt} = \frac{\partial \psi}{\partial i}\frac{di}{dt} + \frac{\partial \psi}{\partial \Theta}\frac{d\Theta}{dt}. \tag{3}$$

The phase current is calculated from combination of (2) and (3) as:

$$\frac{di}{dt} = \frac{v - \left(R + \frac{dL(i,\Theta)}{d\Theta}\omega\right)i}{L(i,\Theta)}. \tag{4}$$

The real angular speed is calculated from equation:

$$\frac{d\omega}{dt} = \frac{1}{J}\left(\sum_{j=1}^{m} T_j(\Theta, i) - T_{load}\right). \tag{5}$$

where J is the moment of inertia and T_{load} is load torque.

The SRM is controlled on the base of rotor position Θ, therefore it is as following

$$\Theta = \int \omega dt. \tag{6}$$

On the base of this mathematical model a simulation model has been created to solve transients for different control techniques to minimize torque ripple in the SRM under normal operation and fault conditions.

IV. Control techniques of torque ripple minimization in SRM

As it was described, one of the disadvantages of the SRM is its torque ripple which can cause also the noise and these negative performances decrease its using in many applications. Several methods or techniques exist how to decrease this ripple. It can be obtained by special construction design of the SRM or by means of control improving. Here are four control techniques described, simulated and compared for normal operation and fault conditions.

A. *Hysteresis current control of SRM with PI speed regulator*

This technique belongs among the simplest types of SRM control techniques, but it has some disadvantages related with torque ripple. This method does not offer so more possibilities how to decrease ripple. It is limited only to use convenient combination of turn on and off angles for different speed and load. Moreover the result may not have been as it is desired. In order to simulate SRM transients and also faulty state the block diagram of hysteresis current control with PI speed controller was created (Fig. 3).

The calculation of turn on and turn of angles has been done before simulation to minimize torque ripple under different speeds and loads. It has been carried out on in accordance with flow chart to find optimal combinations of these angles. The torque ripple Trip has been calculated as follows:

$$T_{rip} = \frac{T_{\max} - T_{\min}}{T_{AV}}. \tag{7}$$

where $T_{\max}$ is maximal value of the torque, $T_{\min}$ is minimal torque and T_{AV} is its average value calculated as:

$$T_{AV} = \frac{1}{T}\int_0^T t dtime. \tag{8}$$

Where T is time of one period and t is instantaneous torque. In the case of one phase opening, the turn on and turn off angles correction are needed for following phase. In the Fig.2 for example, there are calculated turn on angles for health motor (Fig. 2a) and for the phase n+1 after missing phase n when one phase is opened (Fig. 2b).

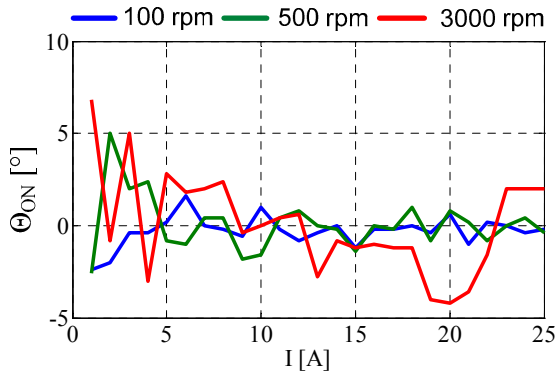

a)

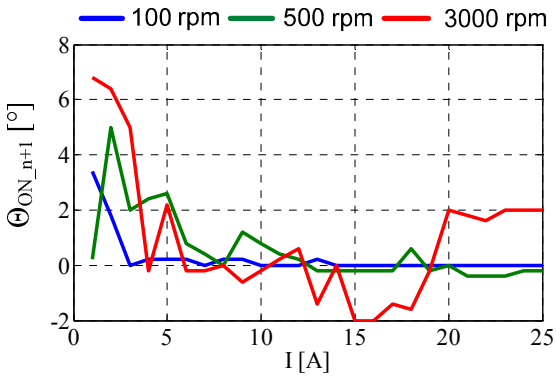

b)

Fig. 2. The calculated turn on angles for health motor (a) and for the fault when one phase is opened (b) for different speed and current.

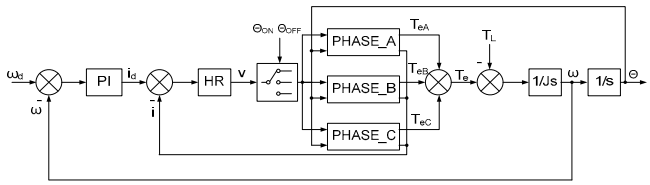

Fig. 3. The block diagram of hysteresis current control with PI speed controller.

The waveforms of current, electromagnetic torque and speed are shown in the Fig. 4. Demanded speed was set to 100 rpm. The load torque 12 Nm was applied in time 3 s and phase *B* fallout (it means, phase B was opened) occurred in time 6 s. During normal operation the minimal torque ripple was reached with turn on and off angles 0° and 21°, respectively. When the faulty state occurred in the phase *B* the turn off angle of the phase A had to be changed to 19° because of producing negative torque, which was originally covered by phase *B*. For higher speeds the turn off angle have to be less than 19°. As it can be seen the torque and speed ripple is very significant for this type of control structure.

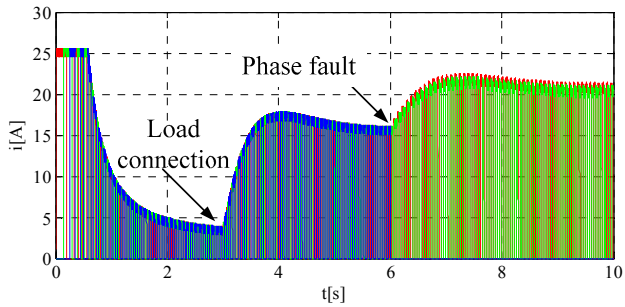

a)

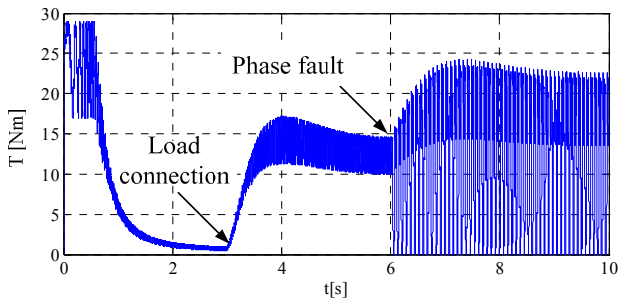

b)

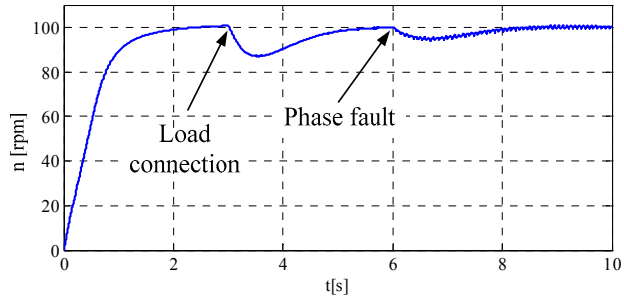

c)

Fig. 4. The waveforms of current (a), electromagnetic torque (b) and speed (c) during start up, load connection and *B* phase opening

B. PWM control technique

This is current control technique with constant switching frequency based on the model of SRM. This method is very similar to hysteresis control method. The block scheme is shown in the Fig. 5. For each PWM impulse relative time switch on is calculated to reach required value of the current [11]. Whole procedure is based on equivalent voltage calculation, which is needed to reach required current in the *k*+1 step. This method is very strictly dependent on the SRM model accuracy and some problems can occur to calculate equivalent voltage because the parameters of the motor can be changed during operation. The principle of this method is shown in the Fig. 6.

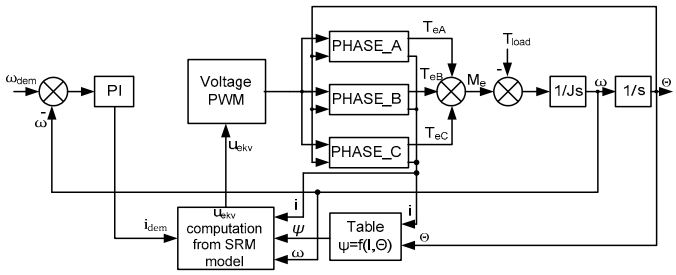

Fig. 5. The block diagram of the PWM technique method.

The waveforms of current and electromagnetic torque are shown in the Fig 13. Demanded speed was set to 100 rpm and the load torque was 12 Nm. The phase *B* fallout (it means, phase *B* was opened) occurred in time 6 s.

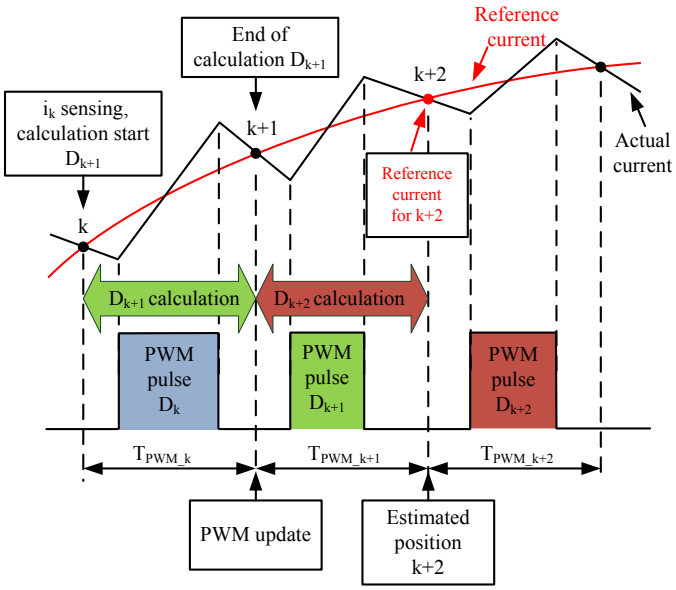

Fig. 6. Explanation of the PWM technique method.

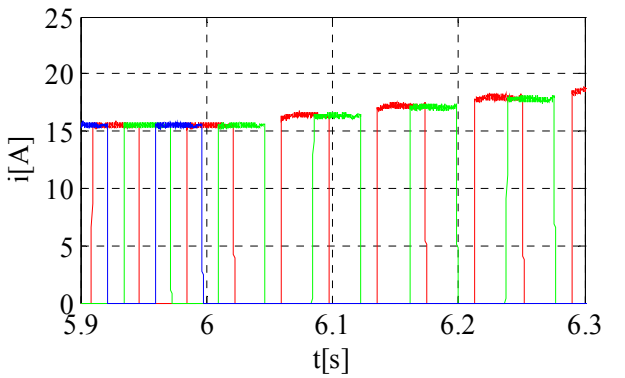

a)

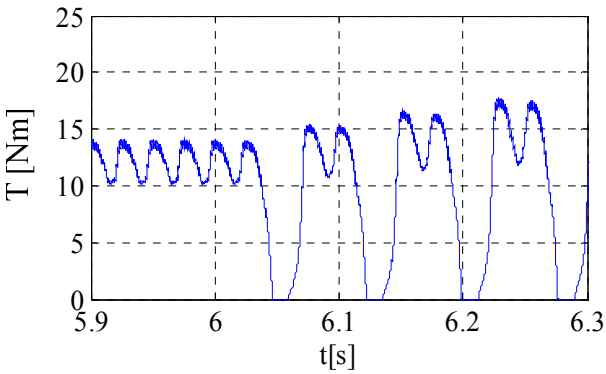

b)

Fig. 7. The waveforms of current (a) and electromagnetic torque (b) of the PWM technique method.

C. *DITC of SRM with current restriction and PI speed regulator*

The DITC is a closed loop instantaneous torque control technique employing a simple hysteresis controller equipped with two hysteresis bands (an interior band and an exterior band) in order to maintain the torque at its reference value within the imposed tolerances. Knowing at each time step the actual current and the rotor position the torque of the SRM can be found by a simple looking in the table. In single-phase conduction, hysteresis controller regulates torque within interior band. During phase commutation, torque of two adjacent phases is controlled indirectly by controlling the total torque within exterior band. The implemented switching strategy is shown in the Table I. Where x means that phase is not used to create the torque. *S* can obtain values as follows: 1 (+Vdc), 0 (0 V) and -1 (Vdc). More details are explained in [12], [13] and [14]. It is very important to remark that DITC needs higher switching frequencies. The disadvantage of DITC is that it can be effectively performed as long as the maximum instantaneous back EMF is equal or less than the dc-bus voltage [12]. The next one is that phase currents are not controlled and it can reach high values, mainly during faulty states when currents in healthy phases are increased to maintain the desired torque. In this case the restriction of current to the value of converter peak current (I_{max}=30 A) has to be done by creating the current control as follows: when the measured phase current reaches the value higher than 29.5 A, the control strategy is switched to hysteresis current control with hysteresis band ±0.5 A. After the decreasing of measured phase current under 29 A the control strategy is changed back to the classical DITC. This intervention can cause decreasing of the torque which can be compensated by accommodation of turn on and off angles for lower speed range. But as it was mentioned above when the faulty state occur the main task is to get the electric vehicle to the nearest service even if the speed is reduced. Block diagram of DITC with current restriction and PI speed regulator is in the Fig. 8.

TABLE I. SWITCHING STRATEGY OF THREE ADJACENT PHASES FOR DITC

Ph n-1 Enable	Ph n Enable	Ph n+1 Enable	Ph n-1 S	Ph n S	Ph n+1 S
0	0	0	x	x	x
1	0	0	1|0	x	x
1	1	0	1|0|-1	1|0	x
0	1	0	-1|x	1|0	x
0	1	1	x	1|0|-1	1|0
0	0	1	x	-1|x	1|0

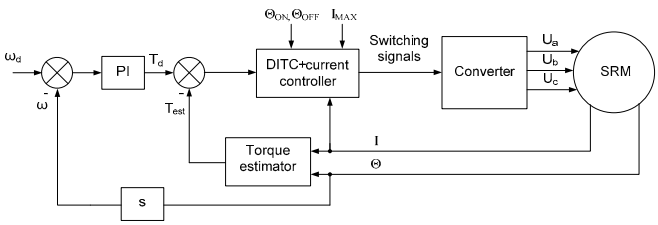

Fig. 8. The block diagram of DITC with current restriction and PI speed controller.

The simulation results of currents, torque and speed can be seen in the Fig. 9. Demanded speed was 100 rpm again. The value of inner and outer torque hysteresis band was set to 0.5 and 1 Nm. The phase *B* fallout occurred in time 6s. Turn on and off angles were computed for normal and for the faulty operation.

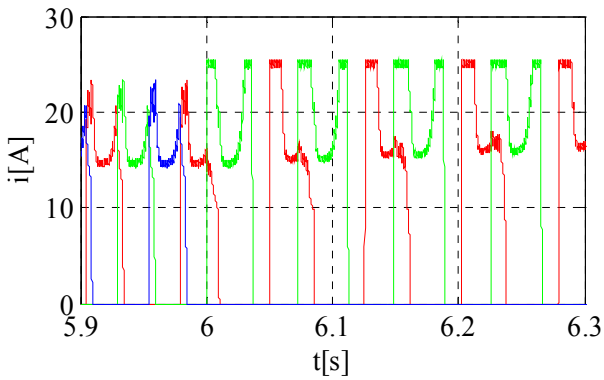

a)

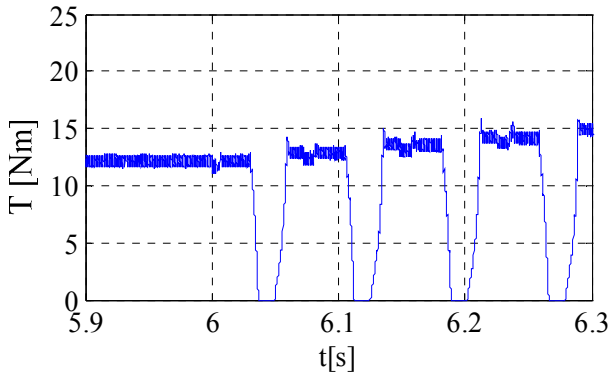

b)

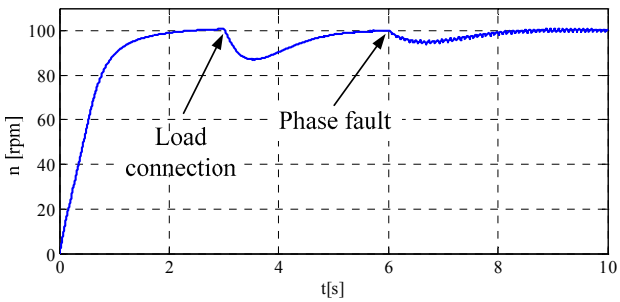

c)

Fig. 9. The simulation results of currents (a), torque (b) and speed (c) for DITC method

D. *Current profiling of SRM*

The last control method described in this paper is current profiling. It means that the phase current waveform is modulated in such a way to reach smooth torque without ripple. Several authors in [15] or [16] deal with this method and applied it in SRM to decrease its torque ripple. The current profiles are calculated in offline regime and saved into table as current versus torque and rotor position I=f(T,Θ). The actual value of the torque is interpolated from existing values for given time. It could take more memory in the processor. For current profiles calculation the static torque characteristics have been used from measurement because of accuracy of this method. In the Fig. 10, there are shown calculated current and torque profiles for each phase and the total torque. It is given for health SRM and speed 100 rpm. In the 11, there is comparison of current profiles for different speeds.

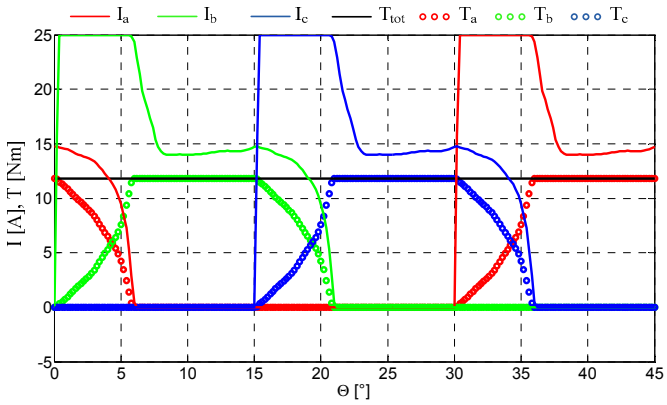

Fig. 10. The calculated current and torque profiles for each phase and the total torque

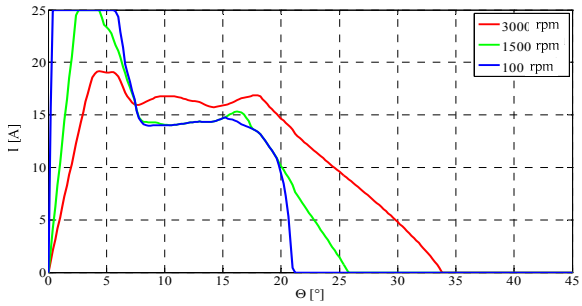

Fig. 11. The comparison of current profiles for different speeds

In the Fig. 12, there are shown the current and torque calculated waveforms when the fault is occurred. In this case, phase *C* is opened and the current profiles generate torque with minimal ripple.

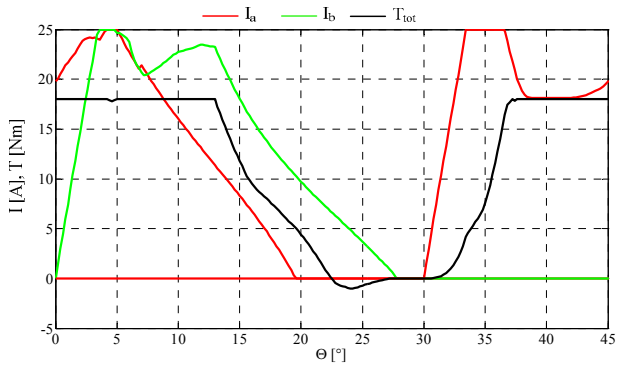

Fig. 12. The calculated current and torque profiles when one phase is opened

The block diagram of this method is in the Fig. 13. This diagram consists of phase currents for health motor table, two

phase currents table for one phase open circuit and flux linkage table for equivalent voltage calculation to reach required currents in the next step. For speed control, the PI regulator is used.

In Fig. 14 is given calculated and measured phase current, which is able to follow the calculated current for speed 100 rpm. PWM frequency is set to 10 kHz.

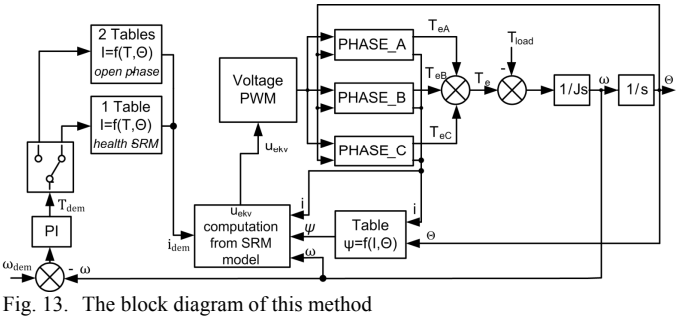

Fig. 13. The block diagram of this method

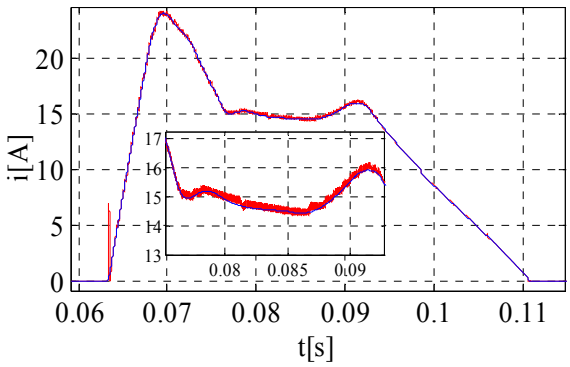

Fig. 14. Ability to follow calculated current profile for speed and PWM frequency 10 kHz for 100 rpm

Finally, the simulation of transients has been carried out for rated torque and several speeds as 100, 500 and 2000 rpm. This method is limited by speed 2000 rpm and torque 18 Nm because both phase currents *A* and *B* reaches their maximal value set to 25 A and the SRM is not able to produce demanded torque for this conditions. It can be seen in the Fig. 18 around the position 5 degrees. The waveforms of the currents, torques and speed are in the Fig. 15. The one phase opening is occurred in the time 6 s.

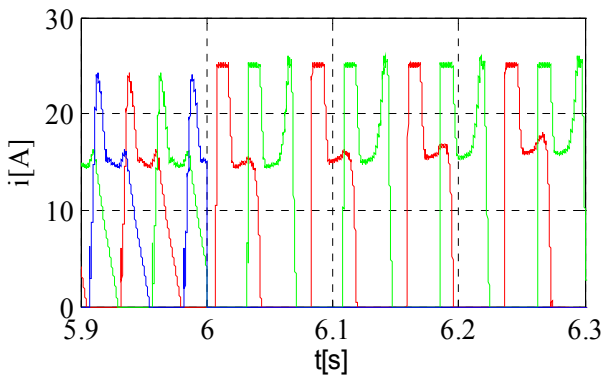

a)

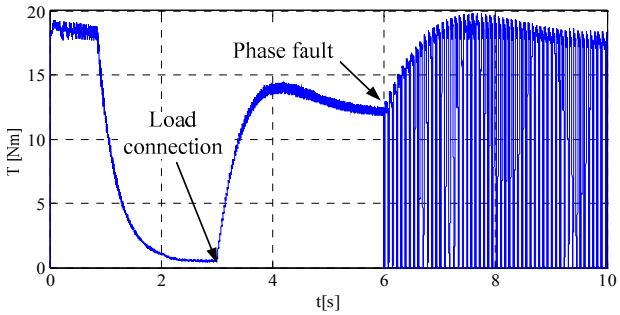

b)

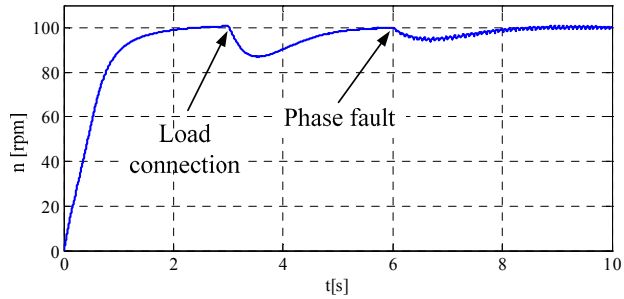

c)

Fig. 15. The simulation results of currents (a), torque (b) and speed (c) for current profiling method

V. Experimental Verification

Several experimental tests were carried out.to verify the simulated dynamic results The SRM converter contains control board equipped with Digital Signal Controller from Freescale (MC56F8346). The experimental test equipment is shown in the Fig.16. The measured waveforms of the currents, torque and speed of the healthy motor and one phase opening were measured for current profiling control method. The speed was kept constant by dynamometer with power 330 kW on 100 rpm. To verify this method, it is necessary to have no speed ripple on the shaft. This is the reason to use dynamometer with very high moment of inertia J=1.9 kg·m^2. In the Fig. 17, there are the phase currents for health SRM (a) and for one phase opening (b). The total torque for health (a) and one phase opening phase (b) can be seen in the Fig. 18.

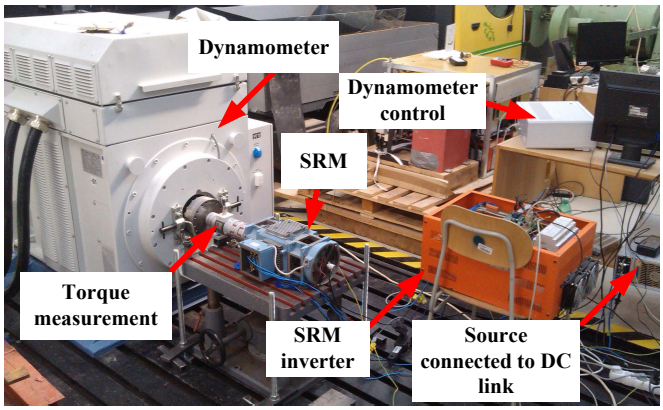

Fig. 16. The experimental setup

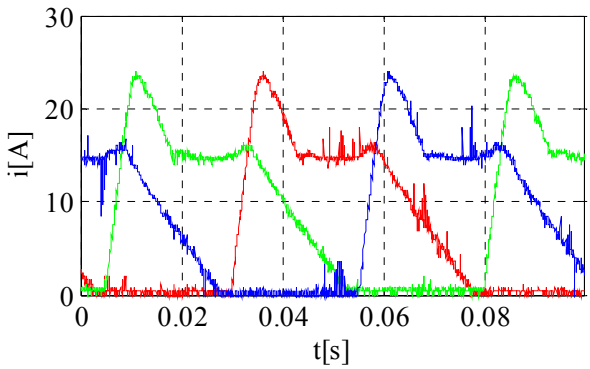

a)

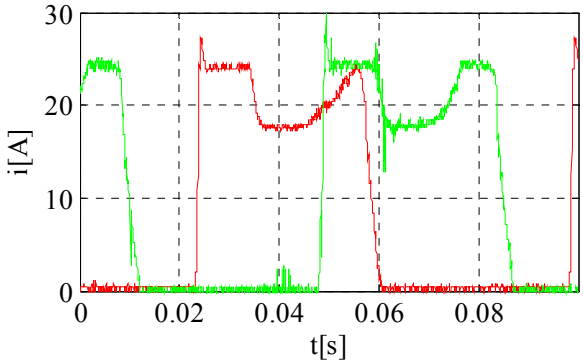

b)

Fig. 17. The comparison of measured current profiles for health SRM (a) and one phase opening (b)

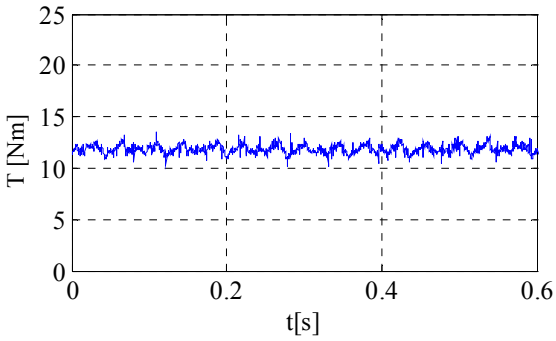

a)

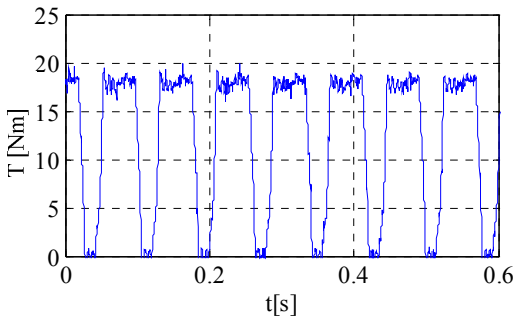

b)

Fig. 18. The comparison of measured total torque for health SRM (a) and one phase opening (b)

VI. Comparison of the Results

The comparisons of all results have been done on the base of equations (7) and (8) for torque ripple definition and average torque calculation. The results are interpreted by bar diagrams for health motor and for one phase opening. In Fig. 19, there is comparison of all simulated methods: blue – hysteresis control of the current, red – PWM control method, green – direct instantaneous torque control and violet – current profiling method. From this figure is clear, that DITC and profiling are the best methods to decrease torque ripple on the minimum value. It could be reached around 5% for 100 rpm and close to 10% for higher speed.

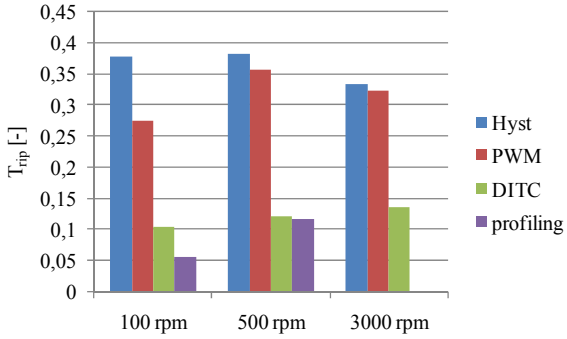

Fig. 19. The comparison of all simulated methods for various speeds for health SRM

In the Fig. 20 is comparison of all control methods for fault state, when one phase is opened: blue – hysteresis control of the current, red – PWM control method, green – direct instantaneous torque control and violet – current profiling method. From this figure is clear, that DITC and profiling are the best methods to decrease torque ripple on the minimum value.

The experimental verification has been carried out for two methods only: PWM and current profiling technique. These results are shown in the Fig. 21 (a) for health SRM and 21 (b) for one phase opening. It can be noted, that the experiments verify very good coincidence of simulated ones and the current profiling method can be applied in the drives with SRM, where smooth torque is needed. The DITC control cannot be verified because the inverter with higher switching frequency (30-40 kHz) is needed to reach adequate results.

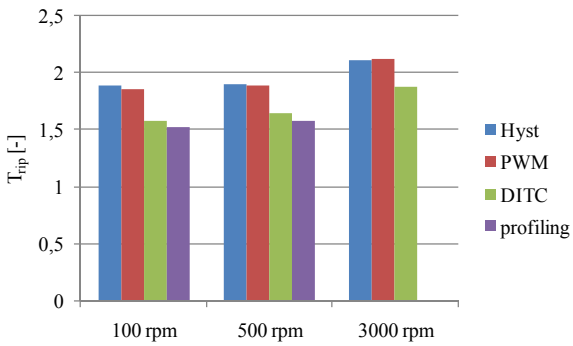

Fig. 20. The comparison of all simulated methods for various speeds and for fault operation of SRM (one phase is opened)

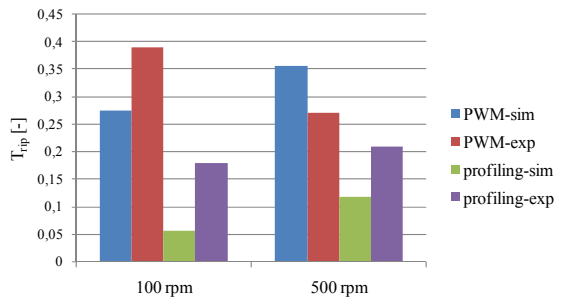

a)

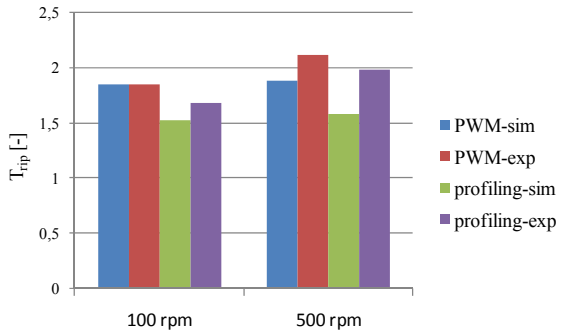

b)

Fig. 21. The comparison of simulated and measured PWM method and current profiling technique for health SRM (a) and fault operation (b) (one phase is opened)

VI. Conclusion

The paper deals with torque ripple minimization in SRM by means of several control techniques which were presented. Investigation of the real SRM static parameter has been done by means of 2D, 3D FEM and compared with measurements. The mathematical model of SRM has been presented to be able simulate transients under normal and fault conditions. Four control techniques have been performed, simulated and several of them also verified by experimental measurements. The best method for torque ripple minimization seems to be current profiling not only for health SRM, but also during one phase opening. This method can be used in the future for control in many industrial applications or electrical vehicles with SRM drive.

Acknowledgment

This work was supported by Slovak Scientific Grant Agency VEGA No. 1/0957/16 and by SRDA No. SK-CN-2015-0007 This paper is supported also by the following projects: University Science Park of the University of Žilina (ITMS: 26220220184) supported by the Research&Development Operational Program funded by the European Regional Development Fund and Centre of excellence of power electronics systems and materials for their components II, No. OPVaV-2009/2.1/02-SORO, ITMS 26220120046 funded by European Community.

References

[1] Miller, T. J. E.: "Switched Reluctance Motors and their Control", Magna Physics, 1992.

[2] Miller, T. J. E.: "Electronic Control of Switched Reluctance Machines", Oxford (U.K.): Newnes, 2001.

[3] Pyrhonen, J., Jokinen, T., Hrabovcova, V.: "Design of Rotating Electrical Machines", John Wiley & Sons, 2008.

[4] Schinnerl, B., Gerling, D.: "*Analysis of Winding Failure of Switched Reluctance Motors*", Proc. of the IEEE Intern. Electric Machines and Drives Conference (IEMDC '2009), Miami, pp. 738-743.

[5] Terec, R., Bentia, I., Ruba, M., Szabo, L., Rafajdus, P: "*Effects of Winding Faults on the Switched Reluctance Machine's Working Performances*", LINDI 2011 3rd IEEE International Symposium on Logistics and Industrial Informatics August 25–27, 2011, Budapest, Hungary.

[6] Gameiro, N.S.; Cardoso, A.J.M. Fault tolerant control strategy of SRM drives, International Symposium on Power Electronics, Electrical Drives, Automation and Motion, SPEEDAM 2008. , pp. 301–306.

[7] Kacenka, V., Rafajdus, P., Makys, P.,Vavrus, V., Szabo, L.: "*Static and Dynamic Fault Analysis of Switched Reluctance Motor*", Intern. conference ELEKTRO 2012, Rajecke Teplice, Slovakia, 2012.

[8] Suying Zhou; Rong Qi, Performance analysis and simulation of switched reluctance motor control system in case of typical faults, International Conference on Transportation, Mechanical, and Electrical Engineering (TMEE), 2011pp. 911–914.

[9] Mir, S., Islam, M.S.,Sebastian, T., Husain, I.: "Fault-Tolerant Switched Reluctance Motor Drive Using Adaptive Fuzzy Logic Controller", IEEE Transactions on Power Electronics, March 2004.

[10] Szabo, L., Ruba, M.: "On Fault Tolerance Increase of Switched Reluctance Machines", EUROCON 2009, pp. 18-23.

[11] R. Mikail, I. Husain, Y. Sozer, Member, IEEE, M. S. Islam, T.Sebastian: A Fixed Switching Frequency Predictive Current Control Method for Switched Reluctance Machines, IEEE Transactions on Industry Aplications, 2014, p. 3717-3726.

[12] Inderka, Robert B; Donker, Rik W.A. A: DITC-Direct Instantaneous Torque Control of Switched Reluctance Drives, IEEE Transactions on Industry Applications, vol. 39, no. 4, July-August 2003, pp. 1046-1051.

[13] Szabo, L., Ruba, M., Fodorean, D., Rafajdus, P., Dubravka P.: Direct Instantaneous Torque Controlled Modular Switched Reluctance Motor Designed for Automotive Applications, 10th International Conference ELEKTRO 2014, Rajecke Teplice, Slovakia, 2014, pp. 239-244.

[14] Dubravka, P.; Rafajdus, P.; Makys, P; Peniak, A., Hrabovcova, V., Szabo, L., Ruba, M.: Design of Fault Tolerant Control Technique for SRM Drive, 16th European Conference on Power Electronics and Applications (EPE-ECCE Europe), Lappeenranta, Finland, 2014.

[15] D.S. Schramm, B.W. Williams, T.C. Green: Torque ripple reduction of switched reluctance motors by phase current optimal profiling, Power Electronics Specialists Conference, 1992. PESC '92 Record., 23rd Annual IEEE, vol.2, p. 857-860, ISBN 0-7803-0695-3

[16] L. Vankatesha, V. Ramanarayan: Torque ripple minimization in switched reluctance motor with optimal control of phase currents, International Conference on Power Electronic Drives and Energy Systems for Industrial Growth, 1998, vol. 2, p. 529-534.

[17] B. Skala, J. Hrusak, D. Mayer, M. Stork, "On Strongly Nonlinear Phenomena in Electrical Machines", New aspect of systems," in N.E. Mastorakis et al., Proccedings of the 2008 WSEAS International Conference. Mathematics and Computers in Science and Engineering (No. 12), Heraklion (Greece), pp. 120-125, 2008.

[18] Stepanek, Jan; Jara, Martin; Drabek, Pavel: Cost-Effective Solution of Input Voltage Stabilizer of Auxiliary Drive Converter for Traction Vehicles, Elektronika ir Elektrotechnika, vol. 21, no. 6, pp. 18-23.